Recognition of pre- and co-seismic electromagnetic signals in magnetotelluric measurements: a case study in the northern region of Algeria

Ahmed Seddik. Kasdi[1,2], Mohamed. Hamoudi[2], Abderrezak. Bouzid[1] and Naïla. Kerbadj[1,2]
[1] Center of Research in Astronomy, Astrophysics and Geophysics, Subsurface Geophysics Division, 16340, BP 63 route de l'Observatoire Bouzarèah, Algiers, Algeria.
[2] University of Science and Technology Houari Boumediene, Department of Geophysics - FSTGAT, BP 32 El Alia Bab-Ezzouar, 16111, Algiers, Algeria.

Summary

Seismo-electromagnetic signals are anomalous electromagnetic (EM) signals related to seismic activity. In recent years, the northern part of Algeria has experienced numerous moderate earthquakes. This seismic activity provided a rare opportunity to study earthquake-related temporal patterns of EM signals using magnetotelluric (MT) measurements. In this paper, we present an analysis of the MT time series using wavelet transform for several cases where co-seismic EM signals were observed. We present the precursor signatures of two main earthquakes using the spectral polarization technique. The results of the wavelet analysis revealed the time-frequency characteristics of the co-seismic EM signal with a high spectral amplitude at different frequency ranges. The spectral polarization technique revealed the existence of anomalies related to the earthquake several hours before its occurrence. This anomaly is correlated with the Dst index. We inferred that the unusual pre-earthquake behavior is related to the precursor signature but not to the solar-terrestrial effect.

Keywords: Northern Algeria, Magnetotelluric, Earthquakes, Seismo-electromagnetic, Time Series Analysis

Introduction

Seismo-electromagnetic signals (SES) have been reported over a wide frequency range (Hattori et al. 2006 and references therein). These EM signals may be precursory (prior to an earthquake) or co-seismic (coinciding with earthquakes). The observation and analysis of these EM phenomena is being used for seismic prediction and to understand the subsurface physical mechanisms related to the generation of these EM signals.

Various physical mechanisms have been proposed to explain the pre-and co-seismic EM signals, such as piezoelectric effect, piezomagnetic effect, microfracture electrification, seismic dynamo effect, and electrokinetic effect (Molchanov and Hayakawa 1998; Ogawa and Utada 2000; Matsushima et al. 2002; Honkura et al. 2002; Huang, 2002; Kasdi et al. 2022). The focal zones are mainly characterized by mechanical deformations, or fracturing generates EM signatures during and before the earthquake in the ULF band (Dudkin et al. 2010).

Previous studies suggest that EM earthquake precursors have emerged as a potential candidate for short-term earthquake prediction (Hayakawa et al. 2007; Dudkin et al. 2010). In this study, we use the spectral polarization technique to identify seismogenic emissions. This method is more flexible with respect to other methodologies that exist for obtaining the precursory signatures (Hayakawa and Hobara 2010).

Northern Algeria is in an active seismic zone in the Mediterranean region. The seismic activity is the result of the convergence between the two main Afro-Eurasian plates. Over the last two decades, northern Algeria has experienced numerous moderate-to-strong earthquakes (Khelif 2019). The recent seismic activity in Northern Algeria provides an opportunity to observe and study SES.

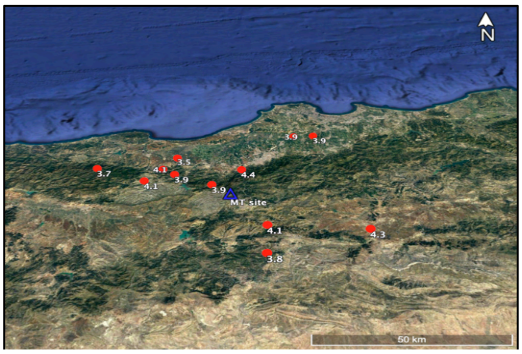

Figure 1. Map of the MT site and the distribution of earthquake epicenters cited in Tab 1.

Observational Database

The geomagnetic observatory of Medea, located about 60 km south of Algiers (Algeria), was chosen to conduct a MT experiment. The MT station was installed in December 2018 (labelled MT-site, Lat: 36.31° N, Log: 2.72° E). The station is equipped with an MTU-A System device from Phoenix-Geophysics. We measured the five components of the EM fields (Ex, Ey, Hx, Hy, and Hz). The sampling rate of the MTU-A is set to 15 Hz. Table 1 summarizes the origin time, position, magnitude, and epicentral distance (d) of earthquakes that occurred near to the MT site where a co-seismic EM signal was observed in the MT time series. Figure 2 illustrates examples of the observed EM signals after the occurrence of the 4.4Mb earthquake cited in Table 1, where t=0 indicates the earthquake origin time. The distinct change in the components of the electric and magnetic fields a few seconds after the earthquake origin time marks a co-seismic EM signal related to the seismic events.

Date	Time	Lat °N	Lon °E	Mag (Mb)	d (Km)
26/09/2018	20:24:35	36.37	2.41	4.1	28.3
29/09/2018	08:00:09	36.35	2.65	3.9	08.6
29/09/2018	14:43:37	36.48	2.52	3.5	27.3
05/11/2018	16:51:56	36.43	2.24	3.7	45.4
12/12/2018	22:11:33	36.60	3.03	3.9	44.5
01/01/2019	04:26:12	36.42	2.47	4.1	26.2
13/05/2019	06:31:57	36.40	2.51	3.9	21.3
19/05/2020	21:06:03	36.06	2.82	3.8	27.7
13/08/2020	**08:04:48**	**36.42**	**2.75**	**4.4**	**14.9**
10/10/2020	15:52:48	36.60	2.95	3.9	40.3
23/12/2020	**18:36:52**	**36.15**	**3.16**	**4.3**	**43.2**
17/01/2021	02:59:56	36.17	2.83	4.1	17.2

Table 1. The location of earthquakes occurred near the MT site (from: https://www.emsc-csem.org).

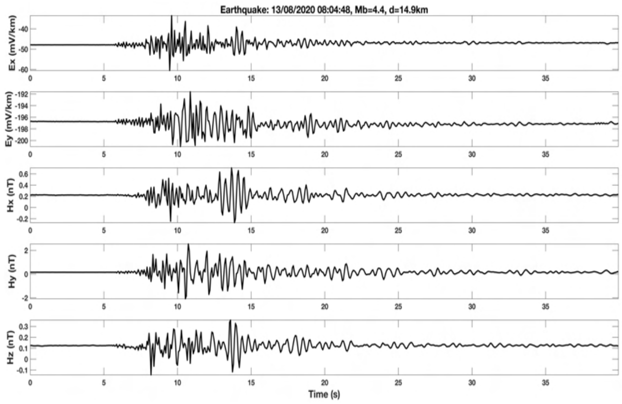

Figure 2. The observed time series data of the five magnetotelluric components measured at the MT site related to the 4.4Mb earthquake.

MT Time Series Analysis Methodology

Wavelet Analysis

Wavelet analysis (Morlet et al. 1982) is a powerful mathematical method in signal analysis that allows one to locate the temporal-frequency change in a time series. The wavelet transforms are further available in two forms, i.e., the continuous wavelet transform (CWT) deals with arbitrarily selected scales, A discrete wavelet transform (DWT) deals with only specific scales. CWT is more appropriate than DWT as it decomposes continuous-time functions into wavelets, whereas, in DWT, wavelets are discretely sampled (Lui and Najmi 1997).

Consequently, we used CWT to obtain the time-frequency representation for the MT time series. The wavelet spectral power values were derived in the 0.05–6 Hz frequency range. As an example, the five component wavelet spectra plots of the MT field signals components related to the 4.4Mb earthquake are presented in Figure 3.

Spectral Polarization Ratio Analysis

The polarization method is based on the measurement of the ratio of spectral power of the vertical magnetic field to the horizontal magnetic fields. This ratio is known to provide us with a lot of information, whether the observed variation is of ionospheric origin (or solar-terrestrial effect) or seismic-related. The polarization ratio analysis, has been demonstrated by prior studies to be effective, especially in the ULF range (Hayakawa et al. 2007; Yusof et al. 2019).

The procedures of the spectral polarization ratio analysis are briefly described. Hourly data is examined and a Fourier transform is applied to each hourly window. The method is repeated for the entire duration of the data set. We used a hamming function for windowing. The FFT transforms time-domain data into the frequency domain in terms of a power spectral density (PSD). The PSD spectrum was obtained in the frequency ranges between 0.05 and 1 Hz. The values of the amplitude spectra were averaged to attain an hourly mean (μ_{hourly_mean}). The normalization approach was implemented on the observation of the total duration of the data considered for this analysis to remove cyclic or daily variations. The standard deviation (σ_{std_td}) of the total duration of observation along with the mean of the data set (μ_{mean_td}) calculated for obtaining the normalized hourly value. The normalized hourly value $(N_{hour,k})$ calculated by using the above values is as follows;

$$N_{hour,k} = \mu_{hourlymean,k} - \mu_{mean\_td,k} / \sigma_{std_{td},k} \quad (1)$$

Here, k represents the three different geomagnetic field components (Hx, Hy, and Hz). 'td' refers to the total duration of data considered for this analysis. The spectral polarization ratio can be calculated using the following formula:

$$P_{Z/G} = N_{hour,H_z} / \sqrt{N^2_{hour,H_x} + N^2_{hour,H_y}} \quad (2)$$

Here, G indicates the total horizontal field components $(G = \sqrt{H_x^2 + H_y^2})$.

The spectral polarization ratio of different magnetic components shows an anomalous behavior before the earthquake (Yusof et al. 2019; Vijaya Kumar et al. 2021).

The spectral polarization technique has been implemented on the magnetic time series for two earthquakes, 4.4Mb and 4.3Mb mentioned in Table 1, respectively. The magnetic data is analyzed for earthquake precursors in the frequency band 0.05–1 Hz. The magnetic data was analyzed to determine the temporal variations of $P_{Z/G}$.

Geomagnetic index

In order to eliminate the effects of global geomagnetic activity and avoid false precursory signals, this study used a global geomagnetic index, namely the disturbance storm time (Dst) index, recorded during the same observation period. The Dst index is used to understand the difference between quiet and disturbed geomagnetic ambiance (Borovsky and Shprits 2017). The Dst index is derived on a one-hour basis from the H component measured by geomagnetic observatories at the middle to low latitudes. The Dst index was taken from the World Data Centre (Nose et al. 2015). A Dst index of less than -30 nT indicates solar activity known as a geomagnetic storm (Gonzalez et al. 1994).

Results and Discussion

The time-frequency representation obtained from the CWT supports the existence of co-seismic EM signals related to the seismic events. The analyzed MT components exhibit spectral enhancement in the frequency range of 2 Hz to high frequency (6 Hz in our case) for all of the earthquakes listed in table 1. The enhancement in the spectral content starts after a few seconds (8 to 15 seconds) of the onset of the mainshock of the earthquake. The increase in the spectral content after the mainshock depends on the epicenter distance as well as the magnitude of the earthquake.

Figure 4 demonstrates the hourly polarization ratio $P_{Z/G}$ (1st panel) and Dst index (2nd panel) from 10/08/2020 to 15/08/2020 (Fig. 4a) and 18/12/2020 to 24/12/2020 (Fig. 4b). The two earthquakes that occurred on 13/08/2020 (Mb = 4.4) and 23/12/2020 (Mb = 4.3) are represented by the vertical blue line. The threshold value defined $\mu p \pm 2\sigma p$ is consistent throughout the recorded duration. An anomalous peak appeared in the $P_{Z/G}$ panel before 10 and 32 h of the occurrence of the Mb = 4.4 and Mb = 4.3 earthquakes, respectively. We correlated these two peaks with the Dst index, suggesting that a value greater than -30 nT defines non-geomagnetic activity during this time. From these results, it is suggested that the anomalous peaks should be considered as precursors of the two earthquakes.

Conclusions

The installation of a MT station in the northern part of Algeria provided the opportunity to study SES. Co-seismic EM signals were observed during several earthquakes. Wavelet analysis has revealed the time-frequency content of the co-seismic EM signals observed simultaneously in the electric and magnetic field components. In the present work, we try to explain the precursor signatures using the spectral polarization technique. It is observed, for the frequency band 0.05–1Hz, a significant increase in the value of the polarization ratio several hours before the occurrence of earthquakes. After comparing the precursor results of each earthquake with the Dst index, we deduced that the unusual behavior before the earthquake is related to the precursor signatures.

These results will help in understanding the SES associated with earthquake activities in the North Algerian region. This kind of analysis should be carried out for many earthquakes to understand the seismo-electromagnetic phenomena.

Acknowledgements

This research was conducted with the support of the Research Center of Astronomy, Astrophysics and Geophysics (CRAAG, Algeria). Data collection was carried out using Phoenix Geophysics MTU-A system devices belonging to the Geophysics Laboratory (USTHB/Algiers). We thank the Geomagnetic Observatories (Kakioka [JMA], Honolulu and San Juan [USGS], Hermanus [RSA], INTERMAGNET, and many others for their cooperation to make the final Dst index available.

References

Borovsky J E, & Shprits YY (2017) Is the Dst index sufficient to define all geo-space storms? Journal of Geophysical Research: Space Physics, 122(11), 11-543

Dudkin F, Rawat G, Arora BR, Korepanov V, Leontyeva O, Sharma AK (2010) Application of polarization ellipse technique for analysis of ULF magnetic fields from two distant stations in Koyna–Warna seism-oactive region, West India. Nat Hazards Earth Syst Sci, 10:1513

Gonzalez WD, Joselyn JA, et al. (1994) What is a geomagnetic storm? Journal of Geophysical Research: Space Physics, 99(A4), 5771-5792

Hattori K, Serita A, Yoshino C, Hayakawa M and Isezaki N (2006) Singular spectral analysis and principal component analysis for signal discrimination of ULF geomagnetic data associated with 2000 Izu Island Earthquake Swarm. Physics and Chemistry of the Earth, Parts A/B/C, 31(4-9), pp.281-291

Hayakawa M, Hattori K, Ohta K (2007) Monitoring of ULF (ultra-low-frequency) geomagnetic variations associated with earthquakes. Sensors 7:1108–1122

Hayakawa M, Hobara Y (2010) Current status of seismo-electromagnetics for short-term earthquake prediction. Geomat Nat Hazards Risk 1(2):115–155

Honkura Y, Matsushima M, Oshiman N, Baris S, Ito A, Iio Y, Isikara AM (2002) Small electric and magnetic signals observed before the arrival of seismic wave. Earth Planets Space 54(12):e9–e12

Huang Q (2002) One possible generation mechanism of co-seismic electric signals. Proc Jpn Acad Ser B 78(7):173–178

Kasdi AS, Bouzid A and Hamoudi M (2022) Electromagnetic Signal Associated with Seismic Waves: Case Study in the North Central Algeria Area. Pure and Applied Geophysics, pp.1-15

Khelif MFA, (2019) La sismicité récente de la région algéroise. *Phd Thesis. Universite des Sciences et de la Technologie Houari Boumediene* (USTHB, Algeria), (in French)

Lui ATY, & Najmi AH (1997) Time-frequency decomposition of signals in a current disruption event. Geophysical research letters, 24(24), 3157-3160

Matsushima M, Honkura Y, Oshiman N, Baris S, et al. (2002) Seismo-electromagnetic effect associated with the Izmit earthquake and its aftershocks. Bull Seismol Soc Am 92:350–360

Molchanov OA, Hayakawa M (1998) On the generation mechanism of ULF seismogenic electromagnetic emissions. Phys Earth Planet Inter 105:201–210

Morlet J, Arens G, Fourgeau E, & Glard D (1982) Wave propagation and sampling theory—Part I & II: Complex signal and scattering in multilayered media. Geophysics, 47(2), 203-221

Nose M, Iyemori T, Sugiura M, & Kamei T (2015) World Data Center for Geomagnetism. Kyoto-Geomagnetic Dst index

Ogawa T, Utada H (2000) Coseismic piezoelectric effects due to a dislocation: 1. An analytic far and early-time field solution in a homogeneous whole space. Phys Earth Planet Inter 121(3–4):273–288

Vijaya Kumar, PV, Rawat, VS, Patro, PK, Gupta, AK and Babu, N (2021) Assessment and recognition of pre-and co-seismic electromagnetic signatures from magnetotelluric data: a case study from Koyna–Warna seismo-active region, India. Acta Geophysica, 69(1), pp.1-15

Yusof KA, Abdul Hamid NS, Abdullah M, Ahadi S and Yoshikawa A (2019) Assessment of signal processing methods for geomagnetic precursor of the 2012 M6. 9 Visayas, Philippines earthquake. Acta Geophysica, 67(5), pp.1297-1306

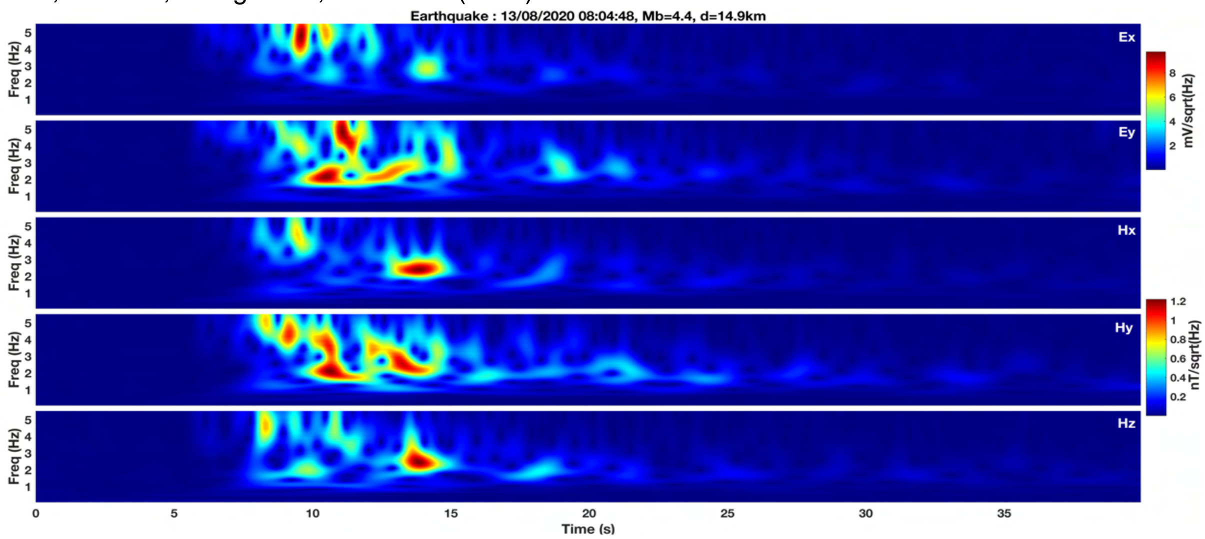

Figure 3. The wavelet power spectrum for the five magnetotelluric components time series data. The time t = 0 is the earthquake origin time. The used wavelet is the Morlet wavelet

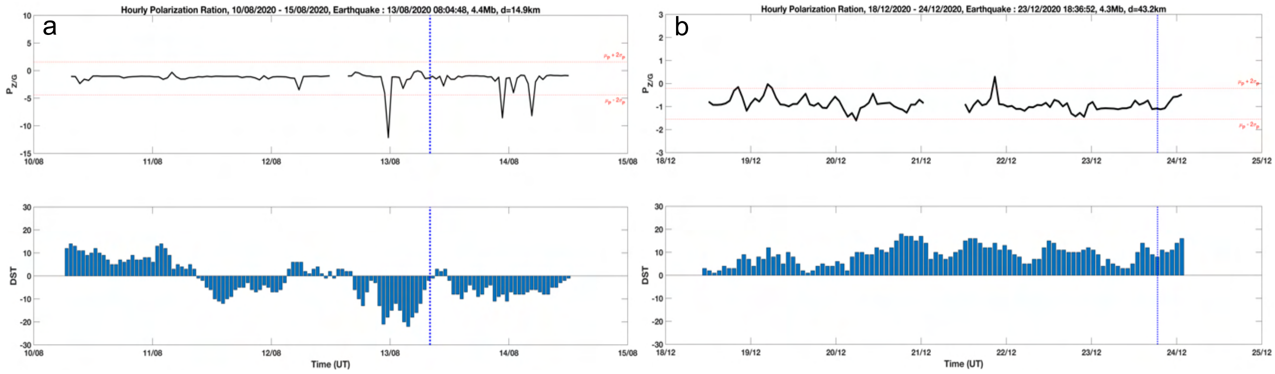

Figure 4. The temporal variation of the hourly spectral polarization of the component $P_{Z/G}$ (1st panel) and Dst index (2nd panel), (a) from August 10, 2020, to August 15, 2020, and (b) from December 18, 2020, to December 24, 2020. The vertical blue line indicates the earthquake origin time (August 13, 2020, Mb = 4.4 and December 23, 2020, Mb = 4.3 for a and b, respectively). The red dashed lines represent the threshold value ($\mu_p+2\sigma_p$) for Δf=0.05–1 Hz.